Available online at www.sciencedirect.com
SCIENCE DIRECT
Journal of Geochemical Exploration 88 (2006) 19–23
JOURNAL OF GEOCHEMICAL EXPLORATION
www.elsevier.com/locate/jgeoexp

Visualization experiments of iron precipitates: Application for in-situ arsenic remediation

M.I.M. Darwish *, V.M. van Beek, J. Bruining

Delft University of Technology, Faculty of Civil Engineering and Geosciences, Mijnbouwstraat 120, 2625 RX Delft, The Netherlands

Received 29 April 2005; accepted 19 August 2005
Available online 26 October 2005

Abstract

Laboratory experiments were carried out to acquire more insight and understanding of the phenomena associated with the in-situ arsenic remediation. Visualization techniques are the most informative for the detection of Fe(II) while flowing in soils. Green Rust (GR) was considered as representative of in-situ iron precipitates. In a visualization flat cell, the change in color of GR to orange, due to oxidation, was monitored by a digital camera and the images were analyzed giving the spatial and temporal distribution of Fe(II). Moreover, both oxygen and pH changes in time were recorded in two sections along the flow direction in the cell. The measured and calculated concentration profiles were compared and the actual reaction rates were predicted. The reaction rate constants measured in this study, under flowing conditions, are in a good agreement with the values obtained from batch experiments reported in the literature.

Keywords: Arsenic remediation; Ferrous iron oxidation; Visualization techniques

1. Introduction

In recent years, the presence of dissolved arsenic in contaminated groundwater from both natural and anthropogenic sources has emerged as a major concern at a global scale (AWWA, 2001). Arsenic (As) is a ubiquitous element present in various compounds throughout the earth's crust. Natural geochemical contamination through soil leaching is the primary contribution of dissolved arsenic to ground waters around the world.

During the in situ arsenic remediation, the aquifer can be considered as a natural subterranean reactor where oxidation and filtration processes for the removal of arsenic and other constituents take place. The injection of oxygenated water displaces iron, arsenic and other water constituents. Thus, an oxidation zone is present in the aquifer where Fe(II) is converted into Fe(III) compounds, which largely precipitate on to the soil grains. During the following production phase, flow is reversed and groundwater flows through the oxidation zone towards the well. Consequently, Fe(II) and As(III) are adsorbed on to the soil grains, which are partially coated by previously deposited oxidation products, e.g. Fe(III) oxyhydroxides. Through the next oxygenated water injection period, the adsorbed Fe(II) is oxidized to ferric hydroxides.

In this paper, we deal specifically with the first stage of the remediation process where the oxygenated water is first introduced in the well vicinity and Fe(II) compounds are oxidized.

* Corresponding author. Tel.: +31 15 278 1641; fax: +31 15 278 6123.
E-mail address: m.i.m.darwish@citg.tudelft.nl (M.I.M. Darwish).

0375-6742/$ - see front matter © 2005 Elsevier B.V. All rights reserved.
doi:10.1016/j.gexplo.2005.08.008

In the field, there are many types of iron compounds depending mainly on oxidation intensity and pH. Under partially oxidizing circumstances (i.e. low dissolved oxygen concentration), part of the dissolved ferrous iron will be oxidized to ferric iron which leads to the formation of GR that precipitates as a sedimentary species that form coatings for soil grains. GR occurs in many soils and sediment systems (Randall et al., 2001). Naturally occurring GR was proved for the first time by Trolard et al. (1997) using Mossbauer and Raman spectroscopes. The aim of this study is to develop a technique to detect the spatial and temporal changes in Fe(II) concentrations that enables the determination of the oxidation rate constants under flowing condition in a porous medium.

2. Methods

For our experiments, we choose GR as a representative of the in situ iron precipitates because it exists naturally and has a color that changes due to oxidation. Thus it can be used to monitor the oxidation process using a visualization technique when the ferrous and ferric iron percentage is well defined. GR is an iron hydroxide compound that occurs under reducing and weakly acid to weakly alkaline conditions as an intermediate phase in the formation of iron oxyhydroxides such as lepidocrocite, goethite and magnetite by oxidation of ferrous iron aqueous solutions (Schwertmann and Fechter, 1994; Vins et al., 1987). They are known as layered double hydroxides (LDH), in which $[Fe_{(1-x)}^{II}Fe_x^{III}(OH)_2]^{x+}$ layers alternate with interlayers made of anions (most commonly CO_3^{2-}, SO_4^{2-} or Cl^-) and water molecules. The green rust that is used in this research is GR II, with the chemical formula $[Fe_4^{II}Fe_2^{III}(OH)_{12}]^{2+}\cdot[SO_4\cdot 2H_2O]^{2-}$ (Genin et al., 1998). When exposed to air, GR is oxidized to either lepidocrocite, goethite or magnetite depending on the rate of oxidation and pH value.

The general oxidation rate of ferrous iron in aquatic ecosystems was defined by Barry et al. (1994). In our study, we focused on the heterogeneous oxidation because it gives the largest contribution to oxidation of Fe(II) to Fe(III) (Wolthoorn et al., 2004).

A visualization technique was adopted to make use of the different colors for ferric and ferrous compounds.

In the literature the iron (II) oxidation reaction rate constants are measured mostly using the batch experiments (Barry et al., 1994; Sharma et al., 2001). In these experiments the iron (II) solution and the selected solids are put together in a beaker while stirring. Thus the reaction rates calculated are not intrinsic since the mass transport contribution is not very well defined as the precise distribution of the solid particles in the solution is not known. Therefore, we choose to measure the oxidation reaction rates under well defined mass transport conditions using a flow in a visualization cell.

The main components of the experimental set-up are: a transparent Perspex cell ($0.8\times10\times20$ cm) packed with glass beads (1.9–2.1 mm diam.) and Clark-style pH and oxygen microelectrodes inserted into the cell, at 8.5 and 15 cm from the inlet. The set-up is installed inside a glove box in which anaerobic conditions are maintained.

The cell was put in the glove box under anaerobic conditions. Oxygen free distilled water was injected at a very low rate while the cell was aligned vertically to avoid gas entrapment. The GR solution was prepared by coprecipitation of Fe(II–III) hydroxysulphate and injected inside the cell. The injection of the GR solution was stopped when the green color in the cell was homogeneously distributed and a break through (i.e. effluent concentration profile) curve indicated equilibrium between the injected solution and adsorption on to the glass beads. Oxygenated water (≈ 8 g/m^3) was injected inside the cell at 0.06 ml/s. pH and dissolved oxygen concentration changes inside the cell were monitored with time. Moreover, the oxidation of GR to Lepidocrocite was recorded via the changes in colors analysing the images of the cell taken with a digital camera. The image analysis was performed by recording the changes in the Red–Green–Blue (RGB) colors.

The mass balances for the three most important elements, namely oxygen, hydrogen, and iron II, can be written as follows with their initial and boundary conditions:

$$\frac{\partial[O_2]}{\partial t}+v\frac{\partial[O_2]}{\partial x}=-1/4k_3'\,A[Fe(II)][OH^-]^2pO_2;$$

$$\left\{[O_2](x=0,t=0)=8\mathrm{g/m^3},[O_2](0<x<L,t=0)=0\mathrm{g/m^3}\right\}$$

$$\frac{\partial[H^+]}{\partial t}+v\frac{\partial[H^+]}{\partial x}=\frac{1}{2}k'_3\,A[Fe(II)][OH^-]^2pO_2;$$

$$[H^+](x=0,t=0)=1\ 10^{-5},$$

$$[H^+](0<x<L,t=0)=1\ 10^{-5}\mathrm{g/m^3}$$

$$\frac{\partial[Fe(II)]}{\partial t}=-k_3'\,A[Fe(II)][OH^-]^2pO_2;$$

$$\left\{[Fe(II)](x=0,t=0)=0\mathrm{g/m^3},[Fe(II)](0<x<L,t=0)=50\mathrm{g/m^3}\right\}$$

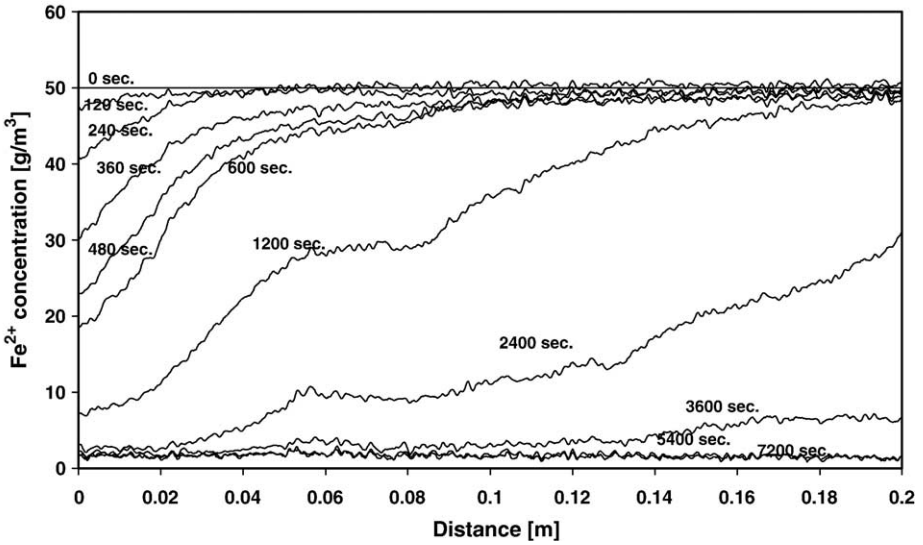

Fig. 1. The spatial distribution of ferrous iron concentration averaged over the cell width, for various times during the injection of oxygenated water.

where A is the available surface area, and L is the total length of the cell. The total iron concentration in the cell, present in the GR, is 75 g/m^3.

3. Results and discussions

The spatial averaged ferrous iron concentration over the cell width was calculated and plotted for various times (Fig. 1).

The measured and calculated (using the above mass balance equations) oxygen concentrations in the cell at two different cross sections are shown in Fig. 2. There is an acceptable agreement between the calculated and measured concentrations except the fact that the measured concentration in the first section is slower than the calculated one. This could be due to some small scale heterogeneity in the GR distribution towards the inlet.

The measured and calculated hydrogen concentrations at two sections along the cell are shown in Fig. 3. We can observe that the shape of the measured and calculated curves is similar but the observed values are several orders of magnitude lower than the calculated ones. This difference could be attributed to the buffer-

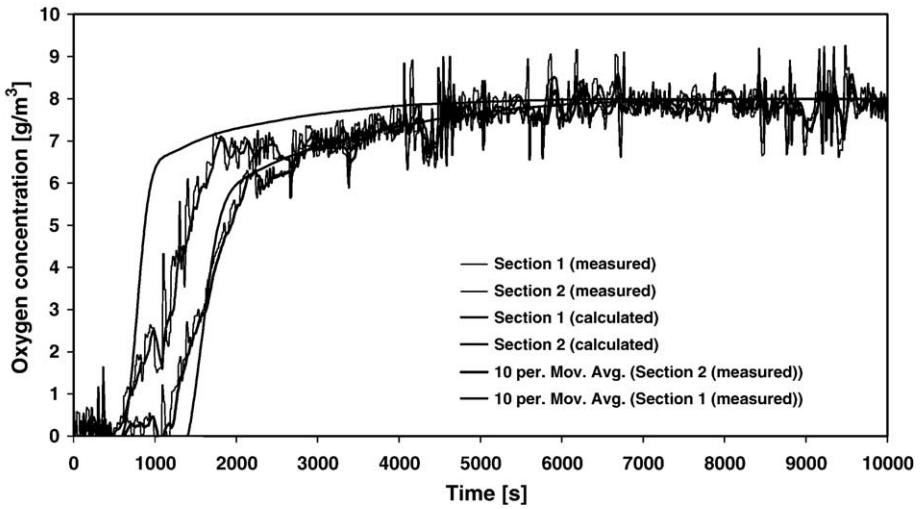

Fig. 2. Variation of the dissolved oxygen concentration vs. time at two different sections along the cell: section 1 and section 2 are respectively located at 0.085 and 0.15 m from the inlet. To smooth the data fluctuations the average of each 10 points was taken as represented by "10 per mov. Avg."

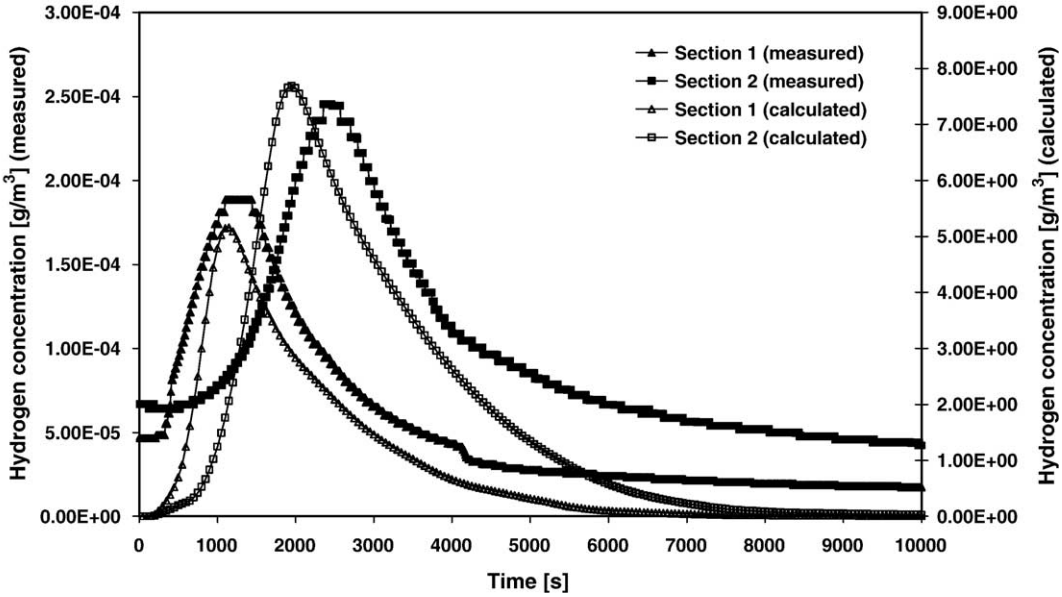

Fig. 3. Variation of the measured and calculated hydrogen concentrations vs. time for sections 1 and 2 (see Fig. 2).

ing capacity of the glass beads present in the cell. The small shift for section 2 could be due to small scale heterogeneities.

Fig. 4 shows the calculated values of the overall heterogeneous oxidation rate constant, divided by the surface area, at two different sections as a function of time. The values are calculated using the ferrous iron mass balance equation knowing the concentrations of oxygen, hydrogen and ferrous iron. At the beginning, the values are high and there is a general decreasing trend except for a short time at the beginning of the experiment. The general decrease in the values could be attributed to the fact that the ferrous iron is scattered in the GR interlayers which results in the occurrence of the "passivation" phenomenon (the formed Fe(III) compounds in outer layers delays the oxidation of Fe(II) in the inner layers. The slight increase at the beginning of the experiments is associated to the

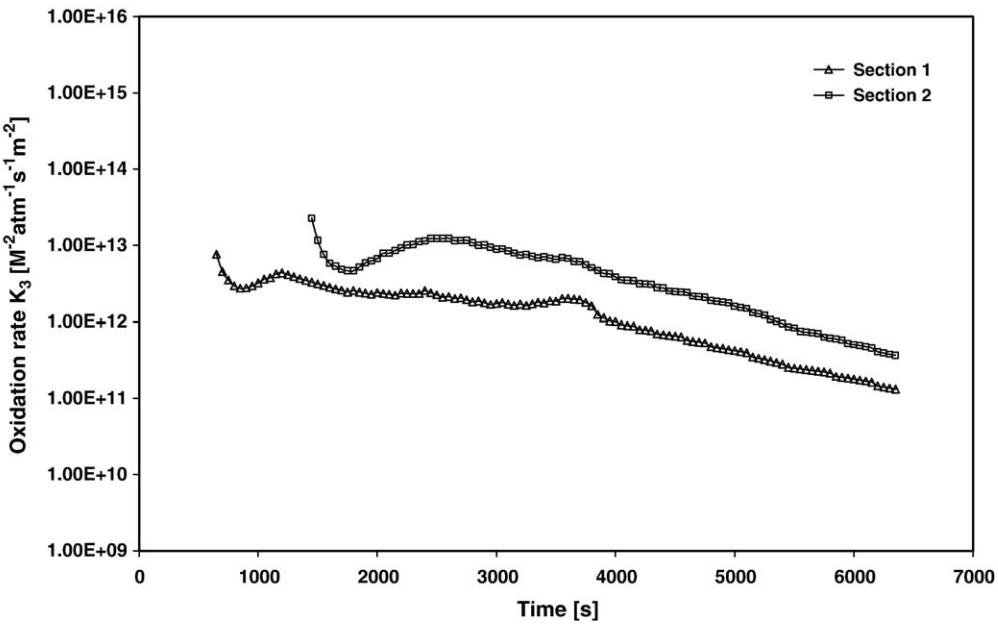

Fig. 4. Variation of the overall heterogeneous oxidation rate vs. time for sections 1 and 2 (see Fig. 2).

lowest pH values since the passivation is less at low pH values. More experiments and modeling are required to validate the preliminary conclusion. The trend of the values at the two sections are parallel which means that the values at the two sections are equal but, that in the second section take place later in time due to flow conditions. The average value is in agreement with the values found in literature (Barry et al., 1994).

4. Conclusions

- Visualization techniques make it possible to determine the in-situ Fe(II) profiles and oxidation rates as a function of space and time.
- The calculated and measured oxygen concentration profiles are in a good agreement quantitatively. Discrepancies between the measured and calculated hydrogen profiles can be attributed to the buffering capacity of glass beads.
- Average values of the actual heterogeneous oxidation rate agree with those found in literature.
- The decrease of the oxidation rate values with time could be explained by the fact that ferrous iron is scattered in the interlayers of the GR and the occurrence of the passivation phenomenon often observed in the field of catalyzed reactions.

References

American Water Works Association (AWWA), 2001. Arsenic rule. Mainstream 45 (2) (February).

Barry, R.C., Schnoor, L.J., Sulzberger, B., Sigg, L., Stumm, W., 1994. Iron oxidation kinetics in an acidic alpine lake. Water Research 28 (2), 323–333.

Genin, J.-M.R., Refait, Ph., Simon, L., Drissi, S.H., 1998. Preparation and Eh–pH diagrams of Fe(II)–Fe(III) green rust compounds. Hyperfine Interactions 111, 313–318.

Randall, S.R., Sherman, D.M., Ragnarsdottir, K.A., 2001. Sorption of As(V) on green rust (Fe_4(II) Fe_2(III) $(OH)_{12}SO_4 \cdot 3H_2O$) and lepidocrocite (γ-FeOOH): surface complexes from EXAFS spectroscopy. Geochimica et Cosmochimica Acta 65 (7), 1015–1023.

Schwertmann, U., Fechter, H., 1994. The formation of green rust and its transformation to lepidocrocite. Clay Minerals 29, 87–92.

Sharma, S.K., Kappelhof, J., Groenendijk, M., Schippers, J.C., 2001. Comparison of physicochemical iron removal mechanisms in filters. Journal of Water Supply: Research and Technology. Aqua 50, 187–198.

Trolard, F., Genin, J.-M.R., Abdelmoula, M., Bourrie, G., Humbert, B., Herbillon, A., 1997. Identification of a green rust mineral in a reductomorphic soil by Mossbauer and Raman spectroscopies. Geochimica et Cosmochimica Acta 61 (5), 1107–1111.

Vins, J., Subrt, J., Zapletal, V., Hanousek, F., 1987. Preparation and properties of green rust type substances. Collection of Czechoslovak Chemical Communications 52, 93–102.

Wolthoorn, A., Temminghoff, E.J.M., Weng, L., van Riemsdijk, W.H., 2004. Colloid formation in groundwater: effect of phosphate, manganese, silicate and dissolved organic matter on the dynamic heterogeneous oxidation of ferrous iron. Applied Geochemistry 19, 611–622.